A Possible Allosteric Communication Pathway Identified through a Resonance Raman Study of Four β37 Mutants of Human Hemoglobin A[†]

Eric S. Peterson and Joel M. Friedman*

Department of Physiology and Biophysics, Albert Einstein College of Medicine, Bronx, New York 10461

Received April 15, 1997; Revised Manuscript Received July 28, 1997

ABSTRACT: The highly conserved tryptophan at position β37 occupies a key locus at the hinge region within the $\alpha_1\beta_2$ interface of the mammalian hemoglobins. This residue is thought to play an important role in mediating the heme−heme interaction associated with the cooperative binding of oxygen; however, its explicit function is unclear. In this study, the proximal heme environments of several β37 mutants of adult human hemoglobin (HbA) are probed using visible (Soret band enhanced) resonance Raman spectroscopy. In the equilibrium deoxy derivatives of these mutants, a systematic variation in proximal strain, as reflected in the iron−proximal histidine (F8) stretching frequency, ν(Fe−His), is seen upon mutation of the β37 residue. The variation in proximal strain correlates with both the ligand binding rates [Kwiatkowski et al. (1998) *Biochemistry 37*, 4325−4335] and conformational changes observed at the FG corner through X-ray crystallography [Kavanaugh et al. (1998) *Biochemistry 37*, 4358−4373]. The results from the deoxy samples indicate a plasticity of the tertiary structure within the T quaternary state. The correlation between the X-ray data and the Raman supports the idea that the proximal strain at the heme within the T state can be modulated by a combination of forces including those arising from the hinge region of the $\alpha_1\beta_2$ interface, from the binding of allosteric effectors, and from the degree of iron displacement from the heme plane. Each of these contributors appears to operate through a shifting of the F helix either away from or toward the FG corner. The Raman spectra obtained from the 10 ns CO photoproduct of the β37 mutant Hb's indicate that these mutants contain an altered coupling between the R state $\alpha_1\beta_2$ interface and the proximal heme environment. This altered coupling could be due to either dissociation of the ligated mutant tetramers into dimers or the formation of an R state tetramer with significantly weakened hydrogen bonds and van der Waals contacts between the α_1 and β_2 subunits at the interface. In either case, the results reveal a clear-cut structural basis for the quaternary enhancement effect in which the normal R state quaternary structure produces a higher affinity ligand binding site than that which occurs in the corresponding dimeric form of the protein. The normal R state interface is shown to be important for stabilizing a favorable ligand binding environment that persists long enough after laser photolysis to enhance the geminate rebinding process within the photoproduct. The addition of IHP to the solution of mutant COHb proteins results in photoproduct spectra that are all identical and are consistent with the ligand-bound derivatives having either a T state structure or a very strained and anomalous R state structure.

Cooperative ligand binding to human adult hemoglobin, HbA,[1] arises largely through a ligation-dependent change in the equilibrium between two quaternary states of the protein (Perutz, 1989; Perutz et al., 1987). At low levels of ligand binding, the low-affinity T state structure dominates, whereas at higher levels of ligand saturation, the high-affinity R state structure is prevalent. Major differences in the structure of the two quaternary states exist within the $\alpha_1\beta_2$ interface. In fact, the large-scale changes in the hydrogen-bonding and salt bridge patterns within this interface are often used to define or identify the quaternary state. The hemoglobin tetramer can be viewed as two $\alpha\beta$ dimers joined through the $\alpha_1\beta_2$ interface, and this interface plays a major role in determining both the stability of the tetramer and the ligand binding properties of the quaternary states (Ackers & Smith, 1985a,b). Furthermore, the binding of a ligand at one site can initiate changes in the $\alpha_1\beta_2$ interface that in turn trigger the onset of tertiary changes and increased ligand affinity at the other sites (Huang & Ackers, 1995; Huang & Ackers, 1996). It is still to be determined which interfacial structural elements influence the dimer−tetramer equilibrium, contribute to the stability of a given quaternary state, and communicate with the ligand binding sites. The present study seeks to explore one such communication pathway by using resonance Raman spectroscopy to probe the proximal heme environment as a function of systematic perturbations of a well-defined region of the $\alpha_1\beta_2$ interface.

[†] This work was supported in part by National Institutes of Health Grants PO1(HL51084) and GM-44343 and also by the W. M. Keck Foundation.

* Corresponding author. E-mail: jfriedma@aecom.yu.edu. Fax: 718-430-8819. Tel: 718-430-3591.

[1] Abbreviations: HbA, human hemoglobin A; IHP, inositol hexaphosphate; β37X, human hemoglobin A with mutations Trp → X, where X = Tyr, Ala, Gly, or Glu, and also Val → Met at position 1 in the β chains; rHbA, recombinant hemoglobin A with the mutation Val → Met at position 1 in the β chains; fwhm, full width at half-maximum intensity.

S0006-2960(97)00869-6 CCC: $15.00 © 1998 American Chemical Society
Published on Web 03/17/1998

In HbA, Trp β37 is in the critical hinge region of the $\alpha_1\beta_2$ interface where significant tertiary structural changes occur with the change in quaternary state upon ligand binding. In both the deoxy T state and the liganded R state, the indole side chain of β37 couples the β_2 subunit to the adjacent α_1 subunit. It remains hydrogen bonded to the Aspα94 and Proα95 across the interface and interacts with the penultimate tyrosine, Tyrα140 (Dickerson & Geis, 1983). In vertebrate hemoglobins, this residue is highly conserved as a tryptophan. These observations and previous work (Ackers & Smith, 1985b) have demonstrated that β37 is one of several residues in the $\alpha_1\beta_2$ interface that plays a key role in the cooperative mechanism and allosteric behavior of HbA.

Several naturally occurring β37 mutants have been isolated and partially characterized: Hb Rothschild (βW37R) (Yamaoka, 1971), Hb Hirose (βW37S) (Gacon et al., 1977; Sharma et al., 1980; Nagai et al., 1995), and Hb Howick (βW37G) (Owen et al., 1993). Hb Rothschild has a reduced oxygen affinity, while Hb's Hirose and Howick have oxygen affinities greater than that of HbA. Two additional mutants, βW37F and βW37T, have been expressed in *Escherichia coli* (Ishimori et al., 1992; Vallone et al., 1996). Because of the apparent variety of effects caused by modifications at this site, it was decided to prepare a number of different β37 variants and to carry out a concerted and comprehensive examination of their properties in order to establish the relationship between the structural impact of changes in this amino acid residue and the ensuing alteration of the functional properties of the hemoglobin molecule.

The work presented herein is accompanied by three papers on these mutants that describe (1) the preparation of the mutants and measured kinetic parameters for CO binding to the deoxy state in millisecond stopped-flow experiments and CO rebinding following millisecond and nanosecond flash photolysis, as well as the preparation of a cross-linked derivative of the βW37E mutant using covalently linked dimers of α chains and the kinetic characterization of this cross-linked mutant (Kwiatkowski et al., 1998), (2) the high-resolution structures of the deoxygenated derivatives of all four of these β37 variants (Kavanaugh et al., 1998), and (3) measurements of molecular weights and thermodynamic binding parameters of the equilibria of oxygen binding under a variety of experimental conditions (Kiger et al., 1998).

In this report we present the results of visible resonance Raman measurements on the equilibrium deoxy derivatives and the photoproduct of the CO saturated derivatives of four β37 mutants of HbA: βW37Y, βW37A, βW37G, and βW37E. The data indicate that the β37 residue does indeed play a key role in the interface and that changes of residue size, polarity, or ability to form a hydrogen bond result in sufficient alteration of the protein structure to have a dramatic impact on the local tertiary structure at the heme, which in turn can be related directly to the changes in ligand binding properties. The Raman results for the deoxy T state show that the functionally relevant proximal heme environment within the T state can be systematically tuned by altering the hinge region of the $\alpha_1\beta_2$ interface. These proximal changes are highly correlated with a progressive change in both ligand binding kinetics (Kwiatkowski et al., 1998) and conformation of the FG corners and degree of disorder in the C-termini of the α chains as seen in the X-ray crystallographic study (Kavanaugh et al., 1998). Together, these results are interpreted using a model in which proximal strain at the iron−His linkage contributes to the formation of a barrier to ligand binding. In this model this strain is modulated through changes in the interface, the DPG binding site, and the heme. All of these changes act by influencing the positioning of the F helix. The model readily accounts for the range of ligand binding properties that can be displayed by the T state.

The results for the 10 ns photoproduct of the CO-bound derivatives demonstrate that β37 contributes strongly to the stability and affinity of the tetramer. These results also provide the structural basis for the quaternary enhancement effect upon formation of an intact tetramer from dimers and highlight the role of the $\alpha_1\beta_2$ interface in setting up not only a proximally strained T state but also a *hyperfavorable* (vis à vis the dimers) proximal environment for the liganded R state species.

EXPERIMENTAL PROCEDURES

Mutant Hemoglobins. The *E. coli* expression system for the β chains of the β37 mutants is described in detail in the accompanying paper (Kwiatkowski et al., 1998) and follows the procedures of Hernan et al. (1992). Very briefly, each β37 derivative contained two mutations. The β1 Val was replaced by Met, and the β37 Trp was replaced by Tyr, Ala, Gly, or Glu. The mutant β globins were combined with normal α chains obtained from hemolysates of freshly drawn blood (Doyle et al., 1992) and heme to form intact tetramers. A reference hemoglobin, rHbA, used as a normal Hb standard for comparison to the β37 mutants was prepared in a similar manner but contained only the β1 Val to Met mutation.

Sample Preparation for Raman Experiments. CO derivatives were prepared from oxy stock solutions by passing CO gas over the surface of a 100 μL aliquot in a sealed vial. Deoxy derivatives were prepared by passing N_2 over a 100 μL oxy aliquot and then adding 5 equiv of sodium dithionite with respect to heme concentration. All samples were approximately 0.7−1.2 mM in heme and in 0.1 M bis-Tris-HCl buffer at pH 7.0. In samples containing inositol hexaphosphate, IHP, the IHP was added in a 1.5-fold excess with respect to the tetramer concentration. (If all the tetramers bound one IHP molecule, the free IHP concentration would be ~125 μM.) The IHP was obtained as the sodium salt from Sigma, and the pH of the stock solution was adjusted by titration with the acid form of Amberlite IR 120 resin to permit acidification without the introduction of additional anions, such as chloride. The samples were then loaded under a N_2 atmosphere into quartz sample cells with a 200 μm path length (Helma P/N 124-QS, Jamaica, NY). The front window of the cell was replaced with a sapphire window, which yielded a flatter baseline in the low-frequency region of the Raman spectrum. The sample cell was mounted in a custom brass holder, which was cooled to approximately 10 °C and rotated fast enough such that a new sample volume was interrogated with each laser shot. Photoproduct buildup and artifacts from sample spinning were found to be negligible by varying the spinning rate and by taking visible absorption spectra before and after each experiment.

Raman Apparatus and Data Analysis. Visible time-resolved resonance Raman spectra were obtained using an

8 ns 435.8 nm pulse to both photodissociate the ligand and Raman scatter off the sample. The laser used was a Nd:YAG laser (Continuum NY81C-20, Santa Clara, CA), which produced 450 mJ pulses at 20 Hz in the second harmonic output at 532 nm. Four watts of the 532 nm beam was focused into a homemade 90 cm long cell filled with 120 psi of hydrogen to Raman shift the laser to 435.8 nm. (Note that in some of the RR spectra a tiny peak at ~180 cm^{-1} appears that is a hot rotational line from the H_2 cell that has not been adequately filtered out and is not a Raman line from the sample.) Neutral density filters were used to reduce the energy of the 435.8 nm pulses to 150 μJ, and these were focused with a 150 mm plano-convex lens on the sample at an incidence angle of 45°. The Raman scattered light was collected at normal incidence to the sample (135° to the laser) with a 50 mm Nikon F/1.4 camera lens and focused with an f-matching lens onto the 50 μm × 5 mm slit of a 0.64 m single monochromator utilizing 1800 grooves/mm grating (ISA HR640, Metuchen, NJ). The Rayleigh line was reduced in intensity with a holographic notch filter that was angle tuned to remove the scattered laser light (Kaiser P/N HNF-1171 centered at 442 nm at an incidence angle of 14°, Ann Arbor, MI). Intensity artifacts created by polarization dependent grating reflectivity were eliminated with a depolarizer used to scramble the polarization of the collected light (CVI P/N DPL-10, Putnam, CT). The detector was an intensified diode array run in the cw mode (Princeton Instruments P/N IRY-1024S/B, Trenton, NJ). The total accumulation time per spectrum was typically 30 min. The spectral bandwidth of the monochromator was approximately 2.5 cm^{-1}, and the resolution of the detector array was approximately 0.9 cm^{-1} per pixel.

Raman spectra were calibrated using solvent spectra with previously determined peak assignments. A least-squares fit was used to map pixel number onto relative wavenumbers (Raman shift). The absolute frequencies in the calibration of the Raman spectrum are accurate to ±0.5 cm^{-1} based upon comparisons with literature values, but frequency differences within a given spectra or between spectra run on the same day can be much more accurate since they share the same calibration. We estimate that relative shifts as small as 0.2 cm^{-1} are significant based upon repeated scans of the same sample and upon the position of the sharp (<5 cm^{-1} fwhm) sapphire line at ~417 cm^{-1} in the spectra of different samples. The Raman spectra were baselined using a polynomial fitting routine in LabCalc and are presented without smoothing (Galactic Industries, Salem, NH). The ν(Fe−His) peak at approximately 216 cm^{-1} in the deoxy spectra was fit to two Gaussians with a 20 cm^{-1} full width at half-maximum intensity to deconvolve the relative contributions of the α and β subunits. The typical reduced χ^2 value for the fit was 1.5. (Note: the noise in the traces is not shot noise limited but rather due to pixel to pixel variations in the response of the intensifier on the ccd device.) The true band profile of the ν(Fe−His) mode is not a Gaussian but is most likely a sum of many Lorentzians (4−5 or a more complicated continuous distribution) (Gilch et al., 1993) which cannot be uniquely fit and interpreted using only the present data. Two peaks were the minimum needed to fit the data and interpret the results within the context of this work and that presented in the accompanying papers. While it is very likely true that multiple conformations exist for both the α and β chains, additional data from a temperature-dependent study on samples with either cyanomet- or metal-substituted hemes would be necessary to adequately resolve the contributions of these conformations to the ν(Fe−His) band. Since the ν(Fe−His) band in these spectra lacks discernible inflection points, a unique fit is impossible to obtain if the width, amplitude, and frequency of each component are allowed to float in the fitting procedure. Fixing the peak widths, however, does result in a reproducible and unique fit. The 20 cm^{-1} width was chosen as the minimum width which resulted in a fit with no shoulders apparent in the sum of the two peaks, but the actual width is not crucial to the results presented herein. Fits with widths from 15 to 25 cm^{-1} resulted in the same trends among the proteins, but with slightly shifted frequencies and percentages.

Fitting of the 10 ns photoproduct spectra was not attempted even though the ν(Fe−His) band can certainly be fit with two Gaussians. The primary reason for this is that ν(Fe−His) frequencies of the of α and β chains in the tetramer photoproduct spectra are much closer together than in the spectra of the deoxy state (Ondrias et al., 1982; Scott et al., 1983; Nagai & Kitagawa, 1980; Mukerji et al., 1994), so that it is not clear that in the presence of the large perturbation of the β37 mutations one could always assign the lower frequency component to the α chain and the higher frequency component to the β chain, as was the case in the deoxy spectra. In addition, it is not absolutely clear what fraction of the tetramers have dissociated into dimers in the CO-ligated samples. This seriously complicates the task of fitting the composite peak as it would require four components for each of the chains in the dimers and the tetramers. In addition, the ν(Fe−His) frequencies of the chains within the dimers are within a few wavenumbers of a perturbed R state tetramer with reduced affinity, so these four components would again not be well separated. Furthermore, when IHP is added to these samples, the dimer−tetramer equilibrium is shifted toward the tetramer, which could shift the frequency either up or down, while the R−T transition is shifted toward the T state, which would shift the frequency down. Again, a temperature study with hybrid hemoglobins is necessary to start to unravel all of these potentially competing changes in the frequency of the ν(Fe−His) band.

RESULTS

Resonance Raman Spectra of the Deoxygenated Derivatives of the β37 Mutants. The resonance Raman spectra between 175 and 875 cm^{-1} for the deoxy derivatives of the reference hemoglobin, rHbA (wild-type α chains and βV1M chains), and the four β37 mutants in the absence of IHP are shown in Figure 1. The significant differences in these protein spectra due to the mutations lie in the low-frequency region between 175 and 400 cm^{-1}. In this region the peak at ~215 cm^{-1} arises from the ν(Fe−His) vibrational mode due to the stretching of the bond between the heme iron to the imidazole ϵ nitrogen of the proximal histidine residue in the F-helix (α87 and β92). The ν(Fe−His) mode displays changes in intensity, shape, and frequency with these mutations. The bands between 275 and 400 cm^{-1} show changes in intensity, but not in position, and these have been attributed to modes involving the heme peripheral groups, particularly the propionates (Jayaraman & Spiro, 1996). An

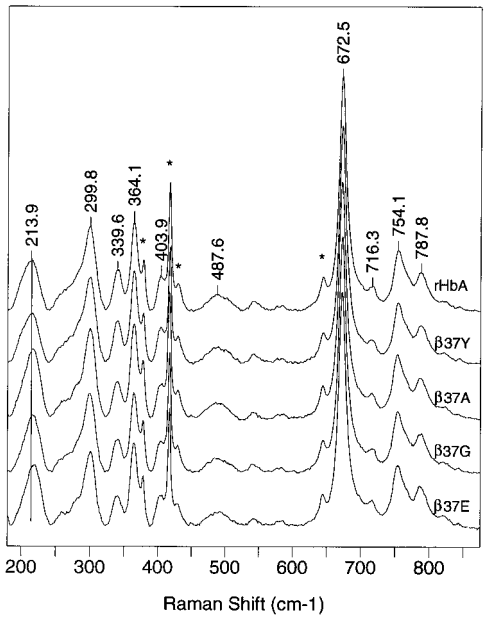

FIGURE 1: Visible resonance Raman spectra of the deoxy reference hemoglobin, rHbA, and the four β37 mutants in the absence of IHP from 180 to 875 cm^{-1}. The spectra were normalized using the ν_7 peak at 673 cm^{-1}. The asterisk indicates peaks from the sapphire window of the sample cell.

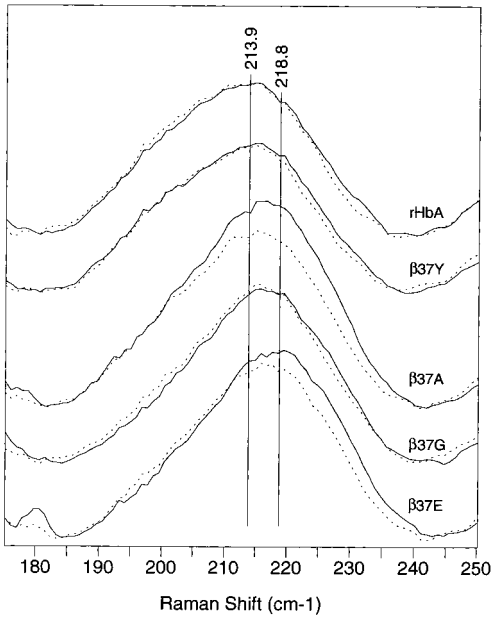

FIGURE 2: Resonance Raman spectra showing the ν(Fe−His) band of the deoxygenated derivatives of the reference hemoglobin, rHbA, and the four β37 mutants in the absence (solid lines) and presence (dotted lines) of IHP. The spectra were normalized using the ν_7 peak at 673 cm^{-1}. The tiny peak at ~180 cm^{-1} in the β37E spectrum is a hot rotational line from the H_2 cell used to frequency shift the laser and is not a Raman line from the sample.

enlarged view of the ν(Fe−His) band for the deoxy proteins in the presence and absence of IHP is shown in Figure 2. The perturbations induced by the binding of IHP are also only evident in the spectra in the low-frequency region of the spectra from 175 to 400 cm^{-1}. The ν(Fe−His) band will be the primary focus of the analysis presented herein.

The line shape of the ν(Fe−His) band was fit as two Gaussians with a 20 cm^{-1} fwhm, and the results are shown in Table 1 along with the position of the maximum intensity,

Table 1: Results from a Curve Fit of the ν(Fe−His) Band in the Deoxy Raman Spectra to Two 20 cm^{-1} fwhm Gaussian Line Shapes[a]

protein	IHP	ω_α (cm^{-1})	A$_\alpha$ (%)	ω_β (cm^{-1})	A$_\beta$ (%)	ω at I_{max} (cm^{-1})
rHbA	−	202	40	217	60	214
	+	201	41	217	59	214
βW37Y	−	201	38	217	62	215
	+	200	38	216	62	215
βW37A	−	204	33	219	67	216
	+	203	36	219	64	215
βW37G	−	205	33	220	67	216
	+	203	31	218	69	215
βW37E	−	206	33	221	67	219
	+	204	34	220	66	217

[a] Estimated errors: frequency, ±1 cm^{-1}; area, ±1%; reduced χ^2 value from the fit, ~1.5.

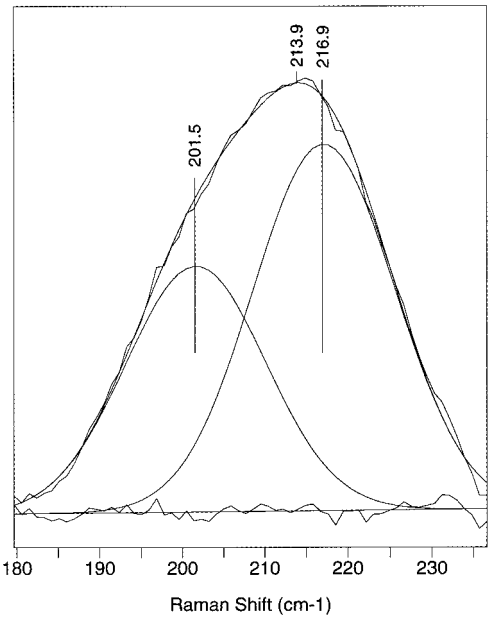

FIGURE 3: Example fit of the ν(Fe−His) band for deoxy rHbA. The line shapes are Gaussians with a 20 cm^{-1} width at half-maximum intensity, and the baseline is linear. Both center frequency and amplitudes were allowed to vary in the fitting procedure. The solid curve through the data is the sum of the two Gaussians.

I_{max}. The use of the two subbands is based on the well-defined difference between the α and β subunits with respect to the peak frequency of ν(Fe−His) in the T state of deoxy-HbA (vide infra). An example of a fit is shown in Figure 3. The I_{max} positions and the frequencies of the two components follow the progression rHbA < βW37Y < βW37A < βW37G < βW37E. It should be noted that the fits are approximations to the true band shape since each chain's ν(Fe−His) band is more complex than a simple Gaussian (Gilch et al., 1993), so the fits do not completely describe all the differences apparent in the spectra. It should also be noted that a peak shift of the ν(Fe−His) band can be achieved both by shifting the frequency of one or both of these two components and/or by changing the relative intensity of one with respect to the other. The βW37Y mutant displays the least perturbation and is nearly identical with the reference wild-type hemoglobin. The difference here is mainly due to a loss of intensity on the low-frequency side of the band. The βW37A, βW36G, and βW37E mutants display much larger differences, and this is due to both a loss of intensity

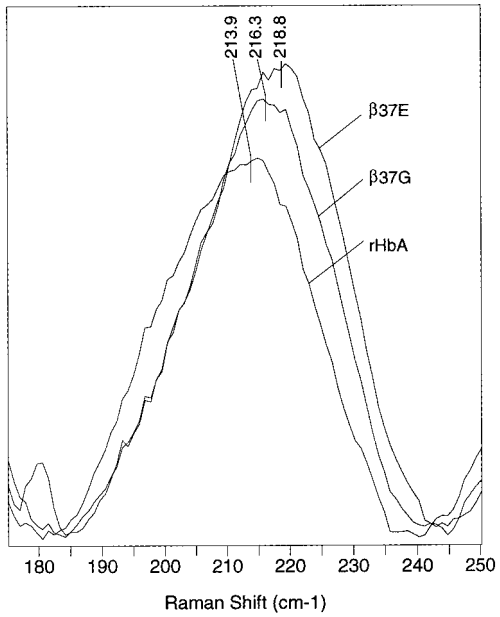

FIGURE 4: Overlap of the ν(Fe−His) bands of the deoxy derivatives of rHbA, βW37G, and βW37E showing the decrease in intensity at the low-frequency edge of the band and the concomitant increase in intensity at higher frequencies due to the mutation. The spectra were normalized using the ν_7 peak at 673 cm^{-1}. The tiny peak at ~180 cm^{-1} in the β37E spectrum is a hot rotational line from the H_2 cell used to frequency shift the laser and is not a Raman line from the sample.

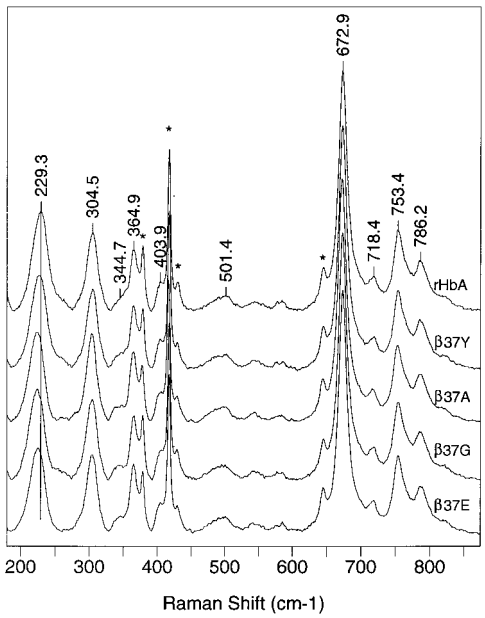

FIGURE 5: Visible resonance Raman spectra of the 10 ns CO photoproduct of the reference hemoglobin, rHbA, and the four β37 mutants in the absence of IHP from 180 to 875 cm^{-1}. The spectra were normalized using the ν_7 peak at 673 cm^{-1}. The asterisk indicates peaks from the sapphire window of the sample cell.

in the low-frequency component and an upshift in both subbands.

The addition of a 1.5-fold excess of IHP with respect to the tetramer concentration (resulting in ~125 μM free IHP if all tetramers bind one IHP molecule) either has no effect or decreases the frequency of the ν(Fe−His) band. The progression of the effect of the mutations at β37 remains the same as in the samples without IHP. To evaluate what changes actually occurred in the ν(Fe−His) band both with and without IHP, several means of comparison were utilized. The two Gaussian fits of the data gave some indication of the band changes, but since the band is not a true Gaussian, this was approximate. A much clearer visualization of the changes could be obtained by overlapping the bands using the LabCalc software after normalizing the spectra using the ν_7 mode at 673 cm^{-1} (Figures 2 and 4). The ν_7 band does not change intensity with these mutations, as can be verified by the excellent overlap of most of the Raman peaks in the spectrum from 400 to 1000 cm^{-1} after this normalization (overlap not shown). The rHbA and βW37Y mutant exhibit a barely detectable frequency downshift in the ν(Fe−His) band and no change in intensity with the addition of IHP. The βW37G mutant shows a slightly larger decrease in frequency in both the high- and low-frequency components, but again the overall intensity of the band does not change. The βW37A and W37E mutants exhibit a small downshift in frequency of both and a loss of intensity in the high-frequency component.

Resonance Raman Spectra of the 10 ns Photoproduct of the CO Derivatives of the β37 Mutants. The resonance Raman spectra from 175 to 875 cm^{-1} of the 10 ns photoproduct of the CO derivatives of these hemoglobins are shown in Figure 5. As has been seen previously (Friedman, 1994; Jayaraman, 1996), the characteristic changes from ligation are evident in these spectra. The ν(Fe−His) band for the rHbA appears at 229 cm^{-1}, the propionate bands at 299 and 365 cm^{-1} shift slightly, the band at 340 cm^{-1} in the deoxy spectra disappears, and a slight shoulder at 345 cm^{-1} becomes evident. As was the case for the deoxy derivatives, the significant differences due to the mutations all occur in the low-frequency end of the spectra between 175 and 400 cm^{-1}. Upon mutation, the ν(Fe−His) band shows further changes in intensity, shape, and frequency, while the propionate bands show only an intensity change. In addition, perturbations induced by the binding of IHP are also primarily evident in the spectra in this low-frequency region. Again, the focus of this work will be on the ν(Fe−His), which occurs near 227 cm^{-1} in these photoproduct spectra. An enlarged view of the ν(Fe−His) bands of the photoproducts with and without IHP is shown in Figure 6. For reasons discussed above, we did not curve fit these spectra, but instead the changes are merely described in terms of a shift in the overall peak position (i.e., the frequency at maximum intensity). In the absence of IHP, the following progression was observed: rHbA (229 cm^{-1}) > βW37Y (227 cm^{-1}) > βW37E (225 cm^{-1}) ≥ βW37A (224 cm^{-1}) = βW37G (224 cm^{-1}). The addition of a 1.5-fold excess of IHP with respect to the tetramer concentration resulted in an ν(Fe−His) frequency of 225 cm^{-1} for the rHbA and a frequency of 222 cm^{-1} for all four β37 mutants.

DISCUSSION

In an earlier study (Ishimori et al., 1992) on the βW37F mutant, the Raman spectrum of a dilute sample of the deoxy derivative yielded a frequency of 223 cm^{-1} for the ν(Fe−His) mode in the absence of IHP. The addition of IHP resulted in a decrease in frequency to ~216 cm^{-1}. The value of 223 cm^{-1} is too high for a normal T state deoxy species based on values obtained for standard T state deoxy hemoglobins (Kitagawa, 1988; Rousseau & Friedman, 1988;

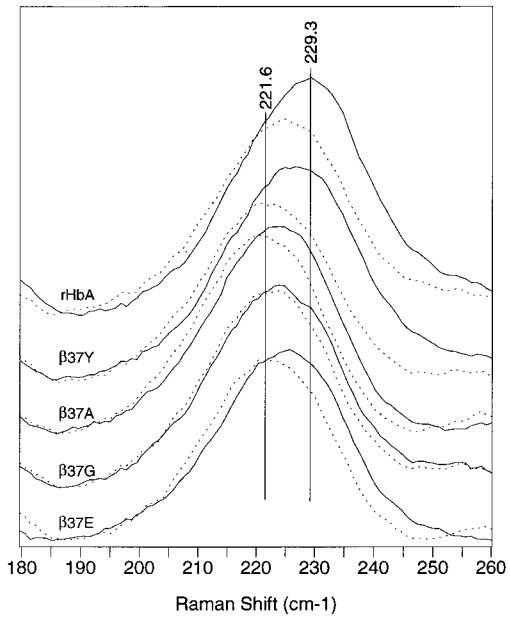

FIGURE 6: Resonance Raman spectra showing the ν(Fe−His) band of the 10 ns photoproduct of the CO derivatives of the reference hemoglobin, rHbA, and the four β37 mutants in the absence (solid lines) and presence (dotted lines) of IHP. The spectra were normalized using the ν_7 peak at 673 cm^{-1}.

Friedman,1994). Nonetheless, an NMR study from this same paper indicated that the deoxy derivative was in fact in the T state. This apparent contradiction was resolved on the basis of the difference in concentrations of the mutant deoxy-Hb used in the two measurements. The NMR study utilized a 1 mM sample (in heme), whereas the Raman study employed a sample that was 2 orders of magnitude more dilute. On the basis of an increase of 6 orders of magnitude in the tetramer−dimer dissociation constant for the deoxy mutant (from 10^{-12} to 10^{-6} M), it was concluded that the Raman measurement had interrogated the deoxy dimer, whereas the NMR had probed the deoxy tetramer. Thus, 223 cm^{-1} is tentatively viewed as the deoxy dimer frequency for ν(Fe−His).

The Raman measurements made in the work presented herein were all made on samples having concentrations (0.7−1.2 mM in heme) similar to what was used for the NMR measurements of Ishimori et al. As a consequence of the concentrations used and the frequencies obtained for the deoxy samples, we conclude that these results reflect the properties of the deoxy T state of the tetrameric form of the mutants [for a general discussion of the ν(Fe−His) mode, see Rousseau and Friedman (1988), and Kitagawa (1988)]. This assumption is supported by the crystallization of all the deoxygenated β37 mutants as tetramers having the T state structure (Kavanaugh et al., 1998). A possible exception to this general conclusion is the frequency of ν(Fe−His) at ∼219 cm^{-1}, obtained for βW37E in the absence of IHP. The enhanced proclivity toward dimer formation in this mutant (Kiger et al., 1998) suggests that a detectable amount of deoxy dimer might possibly be contributing to the spectrum.

The resonance Raman results from the deoxy samples show a progressive increase in the stretching frequencies of the ν(Fe−His) bond for both the IHP-free and IHP-containing samples that follows the same progression that is observed for (1) the increase in CO on rates in the mixing and millisecond photolysis studies (Kwiatkowski et al., 1998) and (2) three specific structural features observed in the X-ray crystallographic data (Kavanaugh et al., 1998). These three structural features are the separation between the $\beta_2$37 residue and the α_1 FG corner, the disorder in the α chain C-terminal penultimate tyrosines, and the iron−proximal histidine ϵ nitrogen bond length.

The overall line shape of the ν(Fe−His) Raman band in deoxy T state hemoglobins is asymmetric largely due to differences between the α and β subunits. It has been suggested that each subunit displays its own heterogeneity that also results in a broadening of this band (Gilch et al., 1993); however, in the deoxy state it has been demonstrated with cobalt−iron (Ondrias et al., 1982) and cyanomet (Nagai & Kitagawa, 1980; Mukerji et al., 1994) hybrids of HbA that the component of the band attributed to the α subunits is a relatively low intensity doublet at ∼202 and ∼212 cm^{-1} and that the component from the β subunits is a more intense band at ∼218 cm^{-1}. The resulting composite band is peaked at ∼214 cm^{-1}. In the present study, the peak position of the entire band increases in the following progression: rHbA < βW37Y < βW37A < βW37G < βW37E. Decomposition of the ν(Fe−His) line shape into the separate contributions from the two subunits (Table 1) and visual overlapping of the bands (Figure 4) suggests that the progressive shift to higher frequency of the ν(Fe−His) mode arises from a shift to higher frequency and decrease in intensity of the α component and a smaller increase in both frequency and intensity of the β component. [Note that the A_i's given in Table 1 refer to the relative area of the bands attributed to the α and β subunits but are not normalized across all the spectra. Thus in a given spectrum, the fraction of one can increase relative to the other, but in comparison to a different spectra, the overall area of the ν(Fe−His) band could have decreased.] These observations of greater spectral changes in the α component are consistent with previous Raman results from studies on HbA including the metal and valency hybrids that have shown that within the frequency range spanned by the T and R states with and without ligands the α subunits display a larger change in both frequency and intensity than do the β subunits (Kitagawa, 1988; Rousseau & Friedman, 1988; Friedman, 1994).

It is significant from a functional point of view that the frequency of the ν(Fe−His) band in the deoxy mutant RR spectra increases in the same protein ordering as do increases in the magnitude of the changes seen in the X-ray structures (Kavanaugh et al., 1998). The implication is that we are observing in the RR spectra a direct impact upon the "proximal strain" at both the α and β hemes as the progressive mutation-induced loosening of the T state constraints propagates through and away from the $\alpha_1\beta_2$ interface into the protein.

"Proximal strain" refers to the strain imposed upon the iron by the protein that makes it energetically more costly to move the iron from an out-of-plane to planar configuration upon ligand binding. On the basis of the deoxy and CO structures of HbA (Baldwin & Chothia, 1979; Fermi et al., 1984; Perutz et al., 1987), one can construct a plausible model, similar to the allosteric core model (Gellin & Karplus, 1977; Gellin et al., 1983), for the mechanism of proximal strain, especially for the α subunits. In the deoxy state, the F helix is shifted toward the EF corner. As a result of this

shift, the imidazole side chain of the proximal histidine is constrained to assume a more tilted position with respect to the heme plane, which in turn increases the van der Waals repulsive interactions between the imidazole carbons and the pyrrole nitrogens. This steric interaction would cause the equilibrium position of the iron atom to move further out of the heme plane and make it energetically more costly to move the iron back into the plane upon ligand binding (assuming the F helix remains fixed). These changes can also result in a change in the tilt and rotation of the imidazole side chain of the proximal histidine with respect to the heme plane and a lengthening and weakening of the iron−proximal histidine bond with a concomitant decrease in the frequency of the ν(Fe−His) mode. Calculations have indicated that the frequency of the ν(Fe−His) mode should decrease with an increase in iron displacement from the heme plane without changing the degree of His tilt (Stavrov, 1993).

Thus, the increases in the frequency of the ν(Fe−His) mode for the deoxy mutants indicates a systematic reduction in proximal strain for the series rHbA < βW37Y < βW37A < βW37G < βW37E, consistent with the reduction of the T state constraints as is clearly seen in the X-ray structures of the deoxy mutants. The mutation results in a gap in the interface as the α_1 FG corner of the β37 mutants pulls away from the $\beta_2$37 residue across the subunit interface (Kavanaugh et al., 1998). If the $\alpha_1\beta_2$ interface is in fact the conduit through which structural changes in one region of the protein are communicated directly to the rest of the protein, one would expect that this increased interfacial gap should result in tertiary changes at the functionally active heme sites.

Overlap of the α subunits of the mutants with the α subunits of the rHbA reveals several additional tertiary structure changes within these mutants. The penultimate tyrosine (α140Tyr) and α141Arg residues in the β37Ala, β37Gly, and β37Glu mutants exhibit anomalously large temperature factors in the crystal structures (increases of 80−400% relative to the rHbA structure). In the wild-type deoxy T state, the α140Tyr is hydrogen bonded to the carbonyl of the α93Val at the FG corner in the same chain and has interactions with the β37Trp and β36Pro residues across the interface (Dickerson & Geis, 1983). In the ligand-saturated R state structure (Shannan, 1983), there is a substantial increase in the temperature factor for the α140Tyr side chain, consistent with a weakening of the hydrogen bond to the Val carbonyl. Further evidence in support of this change in hydrogen bond strength was obtained from a UV resonance Raman study on a cooperative double mutant lacking Tyrα42 (Huang et al., 1997).

An intriguing hypothesis (Huang et al., 1997) is that this hydrogen bond helps to hold the F helix in a position shifted toward the EF corner, thereby contributing to an equilibrium deoxy conformation with higher proximal strain. Thus an increase in the temperature factors for the tyrosine side chain should be accompanied by a shift of the F helix away from the EF corner toward the FG corner (its R state position), a reduction in the tilt of the proximal imidazole, and hence also a reduction in the proximal strain. A previous study (Ishimori et al., 1992) found that the deoxy derivative of the β145Tyr → Phe mutant displayed an increase in both the oxygen affinity and the deoxy ν(Fe−His) frequency with respect to wild type, indicating a decrease in proximal strain but that this protein still remained in the T state with the phenyl ring of the Phe occupying the same site as the ring of the Tyr in the wild-type protein. These authors also point out that mutations which cause a greater perturbation of the structure at this site do cause the β145 side chains to not stay localized within the cleft between the FG corner and the C terminus, but instead to move out into the solvent and become disordered, and that this results in noncooperative R state proteins. Thus, it appears that the loss of the hydrogen bond to the valine without a concomitant large increase in disorder of the penultimate residue is not sufficient to render the protein a noncooperative R state species but does allow the F helix to assume a position closer to its final R state resting point. A similar role is expected for the α140Tyr side chain since both the α140Tyr and the β145Tyr are involved in the same hydrogen-bonding patterns to valine carbonyl groups.

Consistent with the above hypothesis and discussion of the increased α chain C-terminal disorder in the β37 mutants, the overlap of the α chains of the X-ray structures of these mutants does indicate that there is a shift of the F helix slightly away from the EF corner. The perturbation in the F helix can be seen to extend from the FG corner toward the proximal histidine, and the distance that this movement extends down the F helix increases in the proteins in the order β37W < β37Y < β37A < β37G < β37E.

Further optimization of the X-ray structures using a distance geometry algorithm indicates a shortening of the bond length between the histidine ϵN and the iron in the α subunits that again follows the same protein progression as the frequency of the ν(Fe−His) band and the other structural changes described above (Kavanaugh et al., 1998). This same change was found to also occur to a lesser extent in the β subunits. This shortening of the Fe−His bond length is consistent with a strengthening of the bond and the observed increase in frequency in ν(Fe−His). Calculations indicate that a relationship exists between this bond strength and the degree to which the iron atom lies below the average heme plane (Stavrov, 1993). A shortening of the Fe−His bond and a movement of the iron into the heme plane both indicate a decrease in the amount of proximal strain present in the protein structure.

As a last observation from the deoxy data set, The Raman and X-ray data both show a greater amount of change in the α chains than in the β chains upon mutation of the β37 residue. It is not entirely clear why this is the case, though one can simply speculate that the β chain C helix in which the β37 residue resides is more stable to perturbations than is the α chain hinge region containing the FG loop and C-terminus across the interface. From a functional point of view, it is well-known that greater changes occur in the α chains than in the β chains during the quaternary transition and that the α chain hinge region is a major locus for this process.

In summary, the strong correlation between the increase in the frequency of the ν(Fe−His) band in the Raman spectra and the change in the T state constraints in the X-ray structures in the direction of decreased proximal strain within the deoxy state demonstrates that this Raman band can be used as a structural marker for proximal strain in this system. The utility of this correlation is enhanced when it is realized that a correlation also exists between the frequency of the

Table 2: Kinetic Data for the CO Rebinding to the RHbA and the β37 Mutants at pH = 7[a]

protein	IHP	$k_{\text{mixing expt}}$ (10^6 M^{-1} s^{-1})	$k_{\text{photol expt}}$ (10^6 M^{-1} s^{-1})	gem rate (10^6 M^{-1} s^{-1}) [gem yield[d] (%)]
rHbA	−	0.15	5.1 (61) + 0.15 (39)[b]	4.9 [31]
	+	0.09	4.6 (31) + 0.08 (69)	N/A
βW37Y	−	0.24	7.4 (*) + 2.9 (*)[c]	3.4 [23]
	+	0.18	4.0 (20) + 0.16 (80)	N/A
βW37A	−	5.4 (26) + 1.1 (74)[b]	6.0 (*) + 2.3 (*)	2.9 [17]
	+	0.75	4.5 (41) + 1.1 (59)	N/A
βW37G	−	4.6 (32) + 1.5 (68)	5.8 (*) + 2.4 (*)	2.9 [17]
	+	1.0	4.4 (20) + 1.1 (80)	N/A
βW37E	−	5.0 (*) + 2.1 (*)[c]	5.6 (*) + 2.4 (*)	2.7 [17]
	+	1.3	5.3 (47) + 1.7 (53)	N/A

[a] Taken from Kwiatkowski et al. (1998). $k_{\text{mixing expt}}$ is the bimolecular binding rate for a deoxy sample; $k_{\text{Photol expt}}$ is the bimolecular binding rate for a deoxy sample that was prepared from millisecond photolysis of a CO sample. The geminate rate is the first-order rate for rebinding from within the heme pocket after nanosecond photolysis. See text for more details and the significance of each. [b] Amplitude from a two-exponential fit expressed as a percentage. [c] Forced fit to two equal contributions, 50% each. [d] Fraction of ligands that rebind to their original heme in the geminate kinetic phase.

ν(Fe−His) stretching mode and functional parameters connected with ligand binding, such as ligand on rates, geminate rebinding rates (vide infra), and geminate yields (Matsukawa et al., 1985; Friedman et al., 1985; Friedman, 1994). The functional ramifications of this strain and the changes induced by the β37 mutations are described in detail below.

Within the model described above, the functional manifestation of a reduction in proximal strain is a decrease in the barrier to ligand binding. This decrease in barrier height is observed experimentally as an increase in the ligand binding rates. This increase appears to be reflected in the CO on rates measured from pH 6 to pH 8 in the absence of IHP in millisecond stopped-flow mixing and flash photolysis experiments (Kwiatkowski et al., 1998). (The pH 7 kinetic data from Kwiatkowski et al. are retabulated in Table 2 herein for comparison.)

From the kinetic data it is also evident that the trends seen in the Raman and X-ray data correlate with the stability of the tetramer with respect to dissociation into dimers. In both the millisecond stopped-flow mixing and millisecond flash photolysis experiments, the CO binding occurs to the deoxy state, but in the flash photolysis study the sample contains more dimers since it is prepared prior to the kinetic measurements from the CO-bound state in which a significant number of the tetramers have dissociated into dimers. (Micromolar protein concentrations were used in these studies.) The photolysis experiment thus provides both a measure of the kinetic properties of the deoxy dimers and tetramers and also a measure of the stability of the fully ligated tetramer (the CO binding occurs faster than the photolyzed dimers can form tetramers). The fast binding component with a rate constant from approximately 2×10^6 to 7×10^6 M^{-1} s^{-1} is attributed to dimers, while the slower component with a rate of approximately $(0.1-1.0) \times 10^6$ M^{-1} s^{-1} is attributed to tetramers. At pH 7, the mixing data show that both the rates and the fraction of binding that occurs to dimers increase in the order rHbA $\approx$ Y < A < G < E, and the millisecond photolysis data indicate that in the CO-bound state the mutants are wholly dimeric, while the rHbA is ~40% dimeric (by heme).

The IHP effect on the position of the deoxy ν(Fe−His) band is negligible for the rHbA and the βW37Y mutant, whereas there is a small IHP effect in the βW37G mutant, and the βW37A and βW37E mutants are significantly altered. If we assert that the Raman spectra of the deoxy forms of the mutant are reflective of a T state tetrameric species (with the possible exception of the βW37E mutant), then the progression of observed frequencies for the deoxy forms of the different mutants is consistent with the existence of a distribution of available deoxy tertiary conformations within the T quaternary structure. To the extent that proximal strain is reflected in the ν(Fe−His) stretching frequency, a decrease in the ν(Fe−His) is indicative of an increase in proximal strain. It follows that the wild-type and the βW37Y mutant represent an end point for the most strained proximal conformations. This explains why the addition of IHP has minimal impact upon the deoxy spectra of these two species. In the absence of IHP they are essentially already shifted as far as the T state tetramer can go in the direction of increased proximal strain. The βW37A, βW37G, and βW37E mutants have tertiary structures that are not at this high strain limit but have undergone a partial relaxation of the T state constraints, as seen in the X-ray structures, in the same direction as the much larger shift that takes place in the transition to the R quaternary state. As a consequence, the addition of effectors that stabilize the T state can cause a partial reversal of the effects of the mutation: these globins can be "pushed" back into the lower affinity geometry by effectors that favor this more highly strained protein conformation. This reversal is not exact, however, as can be seen in the change in shape of the ν(Fe−His) band in Figure 2. As was discussed above, the mutation primarily affects the low-frequency components from the α chain, whereas the binding of IHP mainly changes the higher frequency components from the β chain. The greater perturbation to the β chain has been observed previously in the binding of IHP to Co/Fe hybrids of HbA (Scott et al., 1983) and is probably due to the fact that the IHP binds directly to the β chain at the DPG site, whereas the changes that then occur in the α chains must be driven by the propagation of the β chain changes through the $\alpha_1\beta_2$ interface. It should be noted that the spectrum of the Glu mutant contains a significant contribution from dimers [approximately 35% of the Raman intensity based on an estimate of $K_{\text{dissociation}} = 1.4 \times 10^{-4}$ and the fact that the Raman intensity is proportional to the heme concentration; $K_{\text{dissociation}}$ for the other deoxy mutants is $\sim 10^{-6}$ and for the reference Hb it is $\sim 10^{-12}$ (Kiger et al., 1998)]. Therefore, the reduction in the frequency of the ν(Fe−His) band for the Glu mutant upon the addition of IHP could be due in part to the decrease in the dimer

population as a result of the preferential binding of IHP to the tetramer. The CO rebinding data for the samples containing IHP from the millisecond mixing and flash photolysis studies are consistent with the Raman results [Table 2 herein and Kwiatkowski et al. (1998)]. Addition of IHP slows rebinding to the tetramer and decreases dissociation of the tetramer into dimers.

The peak frequencies of the ν(Fe−His) bands of the IHP free photoproduct of the βW37G, βW37A, and βW37E mutants are all approximately 224 cm^{-1}. These values are much lower than the Fe−His position of the reference hemoglobin, rHbA, at 229 cm^{-1}. The frequency for βW37Y is an intermediate value of 227 cm^{-1}. The frequency of the ν(Fe−His) mode for the CO photoproduct at 10 ns correlates directly with both the geminate rebinding rate and the geminate yield for the reference hemoglobin and all of the β37 mutants [Table 2 herein and Kwiatkowski et al. (1998)]. The geminate rate characterizes the rebinding of CO from within the heme pocket during the first 10 to few hundred ns after the iron−CO bond is broken, in this case via a 10 ns photolyzing laser pulse. This result directly supports the claim that changes in the frequency of ν(Fe−His) correlate with changes in the barrier height controlling ligand geminate rebinding (Scott & Friedman, 1984, 1994; Friedman et al., 1985; Rousseau & Friedman, 1988).

The correlation between ν(Fe−His) and the barrier height for ligand−iron bond re-formation after photodissociation is made plausible when one considers the sequence of events associated with geminate rebinding. Following the dissociation step, the iron moves out of the heme plane within at most a picosecond or two (Findson et al., 1985a; Petrich et al., 1988; Franzen et al., 1995), and the protein begins to evolve toward the equilibrium deoxy structure. The extent of the initial iron displacement is determined by the tertiary structure of the globin: the more proximal strain within the globin, the greater the iron displacement (Findson et al., 1985a). In HbA, subsequent protein readjustment and further increases of the iron displacement do not begin until many tens of nanoseconds after deligation takes place and progress with time constant ranging from 1 to 20 ms, depending upon the quaternary structure of the initial ligand-bound species (Scott & Friedman, 1984; Hofrichter et al., 1983; Murray et al., 1988a,b; Jayaraman et al., 1995). Thus, within this context, the photoproduct RR spectrum at 10 ns reflects the properties of the five-coordinate heme within the as yet unrelaxed tertiary structure of the initial ligand-bound species. Since geminate rebinding occurs on a time scale (tens of nanoseconds) (Alpert et al., 1979; Duddell et al., 1979; Friedman & Lyons, 1980; Hofrichter et al., 1985) that is faster than overall tertiary relaxation (microseconds), the 10 ns photoproduct spectrum is reasonably reflective of the proximal conformation during the geminate process. Thus, as discussed with the deoxy spectra, the frequency of ν(Fe−His) for the photoproducts is to be viewed as an indicator of proximal strain, i.e., the amount of work against the protein that is required to move the iron in plane upon geminate rebinding. The high frequency observed for rHbA, 229 cm^{-1}, indicates the lowest proximal strain, whereas the value of approximately 224 cm^{-1} for the βW37A, βW37G, and βW37E mutants indicates a greater strain and hence a higher potential energy barrier for geminate rebinding and a reduced geminate rebinding rate, as is observed.

The value of ν(Fe−His) for the photoproduct can also be correlated with the degree of quaternary enhancement reported for these mutants and the reference hemoglobin (Kiger et al., 1998). This quaternary enhancement effect contributes to the cooperativity observed in the ligand binding curve for HbA and can be quantified as the difference in the free energy change between the binding of the fourth ligand to the tetramer and the binding of a ligand to the dimer. Values that are negative imply that the tetramer has a greater affinity for its last ligand than does the dimer, which is uncooperative. The geminate rebinding data and the Raman spectra of the 10 ns CO photoproduct both interrogate the protein under conditions where the effects of the quaternary enhancement mechanism are present since both experiments probe the protein well before the R to T quaternary transition can occur (Hofrichter et al., 1983). Kigar et al. have shown through a determination of the stepwise ligand binding free energy changes that the β37Ala, β37Gly, and β37Glu mutants do not display the quaternary enhancement effect and are either noncooperative or only weakly cooperative. The β37Tyr mutant and the rHbA display both quaternary enhancement and cooperativity.

The implication of this analysis is that under normal circumstances (i.e., in the wild-type tetramer) the R state $\alpha_1\beta_2$ interface actively contributes to changes in the local heme environment that result in an increase in ligand affinity for the binding of the last ligand above and beyond what would be anticipated to occur merely upon the removal of the tertiary constraints imposed by the interface in the T state. In other words, in the R state, the $\alpha_1\beta_2$ interface is not merely passive but is in fact now working in the opposite direction from its function in the T state to create an affinity greater than that which exists in the dimers. The very low value of 214 cm^{-1} of the composite ν(Fe−His) band for deoxy wild-type HbA is a result of interactions along the deoxy T state $\alpha_1\beta_2$ interface, while the value of ∼224 cm^{-1}, as measured for a very dilute solution of deoxy βW37F (Ishimori et al., 1992), is likely to be very close to what would be measured for a deoxy HbA $\alpha\beta$ dimer or tetramer with a nonfunctioning interface. This conclusion follows from the work of Kwiatkowski et al. (1998 and Table 2 in our work) which indicates that addition of IHP results in the re-formation of tetramers in deoxy samples of mutants that have dissociated into dimers. The spectra in Ishimori et al. show a decrease in the ν(Fe-his) frequency from ∼223 to 216 cm^{-1}, a value that is easily assignable to a deoxy tetramer, upon addition of IHP. We have measured a frequency of ∼224 cm^{-1} for the photoproduct of the β37Gly and β37Glu mutants, which, based upon the measured equilibrium constants and the concentrations used in the Raman measurements, are most likely either completely dissociated into dimers or severely perturbed tetramers wholly lacking the cooperative mechanism. Since dimers are regarded as being noncooperative, this value is likely to be at most only a few wavenumbers higher than it should be for a deoxy dimer. Since all three mutants (β37Gly, β37Glu, and β37Phe) show very similar frequencies of ∼223−224 cm^{-1}, it is unlikely that this value is dependent on the identity of the residue at the β37 position. Instead, it is far more likely that this frequency is characteristic of a dimer. Thus, we associate the frequency of 224 cm^{-1} with an altered or nonexistent (as in the case of the dimer) interface in the liganded structure of HbA that is no

longer contributing the extra reduction in proximal strain. Therefore, the correlation between the ν(Fe−His) frequency and proximal strain, the assignment ∼224 cm^{-1} as the ν(Fe−His) frequency of the dimer, and the thermodynamic data all suggest that the increase in ν(Fe−His) from 224 to 229 cm^{-1} is an explicit manifestation of the quaternary enhancement. This *hyperfavorable* (vis à vis the dimers) proximal environment is a consequence of the fully operational $\alpha_1\beta_2$ interface in the liganded R state tetramer.

The observed loss of quaternary enhancement in the βW37A, βW37G, and βW37E mutants can now be explained with either of two possible scenarios: (1) a trivial case in which there is nearly complete dissociation of the tetramers into dimers, which are not cooperative, or (2) a more interesting situation in which the mutation destroys the mechanism that leads to quaternary enhancement within the still associated, albeit loosely, tetramer. This latter scenario also assumes that, for mutants with a marginally functional R state interface, any dissociation into dimers has no observable effect on the geminate rebinding process or on the value of ν(Fe−His). (Note: These two scenarios also explain the geminate rebinding data, as discussed in Kwiatkowski et al. (1998).]

In scenario 1, the data from the millisecond photolysis, geminate rebinding, and 10 ns CO photoproduct Raman studies are all interpretable in a consistent manner by assuming that the liganded forms of the βW37A, β37G, and β37E mutants contain significant amounts of dimer, even at the high concentrations used in the Raman experiments, but that the rHbA and βW37Y mutants remain totally or partially intact as tetramers. This leads to the conclusion that the frequencies of ∼224 and 229 cm^{-1} can be ascribed to the photoproduct of the dimeric and tetrameric liganded species, respectively, and that the value of 227 cm^{-1} for the βW37Y mutant arises from a mixture of dimers and R state tetramers.

Values of the dissociation constants for the tetramer−dimer equilibrium based upon the estimates of the change in free energy associated with this transition (Kiger et al., 1998) suggest that approximately 65−85% of the hemes reside within tetramers at the concentrations of the CO samples used in the Raman experiments. This conclusion would suggest that scenario 1 is not valid and that scenario 2 pertains to the data. In this case, the βW37A, βW37G, and βW37E mutants form tetramers that are so weakly associated that the quaternary enhancement mechanism is not operable. However, this is not entirely consistent with the behavior of the βW37Y mutant. Both the βW37Y and βW27E mutants have the same change in free energy for the formation of ligated tetramers from ligated dimers, yet the Tyr mutant displays quaternary enhancement and the Glu mutant does not.

At this juncture it is not possible to discern which of these two scenarios is operative, and it may well be the case that both are partially in effect. At the sample concentrations used in both the Raman and geminate rebinding experiments, the system is poised near or on the steep part of the tetramer−dimer dissociation curve. As such, a small change in the dimer−tetramer association free energy can produce a large change in the calculated dimer concentration for these samples. Given a reasonably small uncertainty in the measured thermodynamic parameters, it could well be the case that the βW37A, βW37G, and βW37E mutants are nearly completely dissociated in these experiments, while the Tyr mutant remains partially associated and the rHbA remains intact as a tetramer. If this is the case, then the simplest explanation that is consistent with both the Raman and geminate recombination data is scenario 1. This does not, however, preclude a possible role for residue-dependent quaternary enhancement differences due to modulation of the interface strength by the mutations in the tetramers that do exist.

The addition of a slight excess of IHP to the CO derivatives of the mutant species results in a decrease of ν(Fe−His) to the same value of 222 cm^{-1} for all four mutants. For rHbA, the addition of IHP produces a peak at ∼225 cm^{-1}, as previously reported for wild-type HbA (Friedman et al., 1983; Scott et al., 1983). All previous studies indicate that IHP stabilizes the tetramer, and the millisecond CO binding data in the accompanying paper (Kwiatkowski et al., 1998) support this concept as well. Furthermore, it is not likely that IHP binds appreciably to the dimer at the low relative concentrations used in these studies (1.5-fold excess with respect to the tetramer concentration). The photoproduct spectra in the presence of IHP must therefore be attributable to a tetrameric species, and the invariance of the ν(Fe−His) band implies that the heme pocket of this species (with IHP bound) must be relatively insensitive to the mutation at β37. The low value for ν(Fe−His) suggests that either the CO derivative is a high-affinity T state species or a highly strained R state with relatively low affinity. Given the anticipated greater stability of the T state tetramer over the seemingly undetectable R state tetramer for most of these mutants, we are inclined to attribute the low frequency of ν(Fe−His) to a T state CO derivative of the mutants. This conclusion is further supported by the observation (Friedman and co-workers, unpublished results) that the geminate yield for the CO derivatives of the mutants in the presence of IHP is almost zero, as is anticipated for a T state CO derivative (Murray et al., 1988a,b), but not the CO derivative of either a dimer [as is evident in the geminate rebinding results reported in Kwiatkowski et al. (1998) and Table 2 herein] or an R state tetramer. The formation of a T state tetramer upon binding of IHP is consistent with both of the two possible scenarios used above to interpret the CO photoproduct Raman data in the absence of IHP. In scenario 1, the IHP simply causes the dimers to reassociate into T state tetramers, and in scenario 2, either the ligand affinity of the altered R state tetramer is further decreased by the IHP or IHP induces a full R to T transition.

It is interesting that in the presence of IHP the photoproduct of the rHbA has a greater ν(Fe−His) frequency than does any of the mutants. It must be the case that, even in the presence of IHP, a Trp side chain at β37 maintains a unique interaction in the ligated state that results in a higher affinity structure that more closely resembles the unperturbed R state in the absence of IHP and thus has the higher ν(Fe−His) frequency. It appears, then, that the Trp at β37 plays an important role in preventing dissociation of the tetramer into dimers as well as in stabilizing a low-affinity conformation within the deoxy T state and a high-affinity conformation within the liganded R state, both in the absence and in the presence of allosteric effectors.

CONCLUSIONS

In this paper we have presented data from Raman experiments on human hemoglobin, HbA, with mutations of the highly conserved the β37 tryptophan in the $\alpha_1\beta_2$ interface. The Raman data from this study indicate that the proximal heme environment of equilibrium T state deoxy-Hb, including the degrees of freedom reflective of proximal strain, can be tuned by replacing the Trp at the β37 position with other residues. The magnitude of the observed changes increases as rHbA < β37Tyr < β37Ala < β37Gly < β37Glu. These results indicate that there is an inherent plasticity associated with T quaternary state that allows for a large variation of the conformational and functional properties of the ligand binding site within the T state.

The correlation between ν(Fe−His) and X-ray crystallographically determined structural parameters connected with the $\alpha_1\beta_2$ interface indicates that β37 plays a significant role in maintaining the position of the F helix in the T state and therefore also in determining the functional properties of the protein. This role is especially important since the positioning of the F helix appears to be directly linked to the generation of the proximal strain that is the basis of the low ligand affinity in the T state. Consistent with this picture is the correlation between the conformational variables from both the Raman and the X-ray studies and the ligand binding rates of the mutant deoxy-Hb's. The X-ray data implicate two (not mutually exclusive) possible mechanisms through which the mutations at the β37 site could produce changes in proximal strain at the heme. Both of these involve changes that also occur to a much greater extent in the transition to the fully ligated R quaternary structure. One possibility is that the increase in separation between the β_2 37 residue and the FG corner of the α_1 subunit in the mutants is communicated along the interfacial contacts and results in the shift of F helix toward the FG corner. The other possible mechanism is that the mutation causes a weakening of the hydrogen bond between the penultimate tyrosine (α140) and the carbonyl of the α93 valine in the FG loop, which should also allow the F helix to slip toward the FG corner. In either case a shift of the F-helix toward the FG corner is associated with a reduction in proximal strain and a decrease in the barrier to ligand binding that becomes apparent as an increase in ligand affinity.

The addition of IHP, which binds to the DPG site in the central cavity, to the deoxy samples partially reverses the effects of the mutation at β37. Together, these observations suggest that the final disposition of the F helix within the deoxy T state structure is the result of a balance between changes induced by the binding of DPG-type effectors that favor a shift of the F helix toward the EF corner (higher proximal strain) and the loosening of the T state constraints at the FG corner that favor a shift of the F helix toward the FG corner (resulting in reduced proximal strain). In addition, changes in the iron either through ligand binding or replacement with other metals can also influence the shifting of the F helix. Movement of the iron into the heme plane upon ligand binding should favor a shift of the F helix toward the FG corner. This shift is due to the proximal imidazole adopting a less tilted geometry since the repulsive interactions between the pyrrole nitrogens and imidazole carbons increase with decreasing iron displacement (Rousseau & Friedman, 1988; Friedman, 1994). According to Yonetani and coworkers, decoupling the F helix from the heme through either bond rupture or removal of the iron should allow the F helix to shift even further toward the EF corner (Fujii et al., 1993). Thus, these T state "forces" can be present to varying degrees based on solution conditions and the presence of mutations, effectors, and ligands to produce a distribution of both T state tertiary conformations and ligand binding properties.

The frequencies of ν(Fe−His) in the 10 ns CO photoproduct of the β37 mutants indicate either that CO-liganded Ala, Gly, and Glu mutants, and to a lesser degree in the Tyr mutant, do not form an R state tetramer (even at a ~0.20 millimolar protein concentration) or that the resulting R state tetramer has an $\alpha_1\beta_2$ interface that is weakened to such an extent that influence of the R state upon the ligand binding site is severely decreased, resulting in a markedly diminished quaternary enhancement effect. The absence of a quaternary enhancement effect in several of these mutants coupled with the observed ν(Fe−His) frequencies indicates that the quaternary enhancement effect arises through a direct influence of the R state $\alpha_1\beta_2$ interface on the proximal heme environment. The results suggest that the R state functional properties are not just the result of a relaxation of the T state constraints in the individual globin chains, as is seen in the dimers, but that this effect actually arises from the liganded R state $\alpha_1\beta_2$ interface directly enhancing the proximal heme pocket environment and decreasing the barrier to ligand rebinding. In particular, it appears that the R state interface prevents the subnanosecond rapid relaxation of the tertiary structure of the liganded state seen in myoglobin (Findson et al., 1985b) upon ligand dissociation, thereby maintaining a highly favorable environment for geminate recombination.

It should be noted that, given the high degree of conservation among hemoglobins of the residues involved in the hydrogen bonds and salt bridges spanning the $\alpha_1\beta_2$ interface, it is highly likely that there are additional residues besides β37Trp that also play a defining role in determining the properties of HbA.

An important finding in the present work is the correlation of the ν(Fe−His) frequency with ligand binding parameters in the presence of allosteric effectors and upon mutation of the $\alpha_1\beta_2$ interface. The correlation in the deoxy state Hb's is with the ligand on rates, while in the 10 ns CO photoproducts, the correlation is with geminate rebinding rates and yields. These results strongly support the earlier claims linking proximal strain to the ligand affinity and the barrier controlling iron−ligand bond formation.

ACKNOWLEDGMENT

We thank Dr. Robert Noble, Dr. Jeff Kavanaugh, Dr. Alexandra Klinger, Dr. Stephen Sligar, and Kevin Sanders for helpful discussions regarding the data herein and its relationship to the data in the accompanying papers. We thank Dr. Noble and Hilda Hui for providing the samples for the experiments.

REFERENCES

Ackers, G. K., & Smith, F. R. (1985a) *Biophys. J. 49*, 155−165.
Ackers, G. K., & Smith, F. R. (1985b) *Annu. Rev. Biochem. 54*, 597−629.
Alpert, B., El Mohsni, S., Lindqvist, J., & Tfibel, F. (1979) *Chem. Phys. Lett. 64*, 11−16.

Baldwin, J., & Chothia, C. (1979) *J. Mol. Biol. 129*, 175−220.
Dickerson, R. E., & Geis, I. (1983) *Hemoglobin*, p 43, Benjamin/Cummings, Menlo Park, CA.
Doyle, J. L., Lew, G., De Young, A., Kwiatkowski, L., Wierzba, A., Noble, R. W., & Ackers, G. K. (1992) *Biochemistry 31*, 8629−8639.
Duddell, D. A., Morris, R. J., & Richards, J. T. (1979) *J. Chem. Soc., Chem. Commun.*, 75−76.
Fermi, G., Perutz, M. F., Shaanan, B., & Fourme, R. (1984) *J. Mol. Biol. 175*, 159−174.
Findsen, E. W., Friedman, J. M., Ondrias, M. R., & Simon, S. R. (1985a) *Science 229*, 661−665.
Findsen, E. W., Scott, T. W., Chance, M. R., Friedman, J. M., & Ondrias, M. R.(1985b) *J. Am. Chem. Soc.* 107, 3355−3357.
Franzen, S., Bohn, B., Poyart, C., & Martin, J. L. (1995) *Biochemistry 34*, 1224−1237.
Friedman, J. M. (1994) *Methods Enzymol. 232*, 205−231.
Friedman, J. M., & Lyons, K. B. (1980) *Nature 284*, 570−572.
Friedman, J. M., Scott, T. W., & Stepnoski, R. A. (1983) *J. Biol. Chem. 258*, 10564−10572.
Friedman, J. M., Scott, T. W., Fisanick, G. J., Simon, S. R., Findsen, E. W., Ondrias, M. R., & MacDonald, V. W. (1985) *Science 229*, 187−190.
Fujii, M., Hori, H., Miyazaki, G., Morimoto, H., & Yonetani, T. (1993) *J. Biol. Chem. 268*, 15386−15393.
Gacon, G., Belkhodja, O., Wajcman, H., & Labie, D. (1977) *FEBS Lett. 82*, 243−246.
Gellin, B. R., & Karplus, M. (1977) *Proc. Natl. Acad. Sci. U.S.A. 74*, 801−805.
Gellin, B. R., Lee, A. W. M., & Karplus, M. (1983) *J. Mol. Biol. 171*, 489−559.
Gilch, H., Schweitzer-Stenner, R., & Dreybrodt, W. (1993) *Biophys. J. 65*, 1470−1485.
Hernan, R. A., Hui, H. L., Andracki, M. E., Noble, R. W., Sligar, S. G., Walder, J. A., & Walder, R. Y. (1992) *Biochemistry 31*, 8619−8628.
Hofrichter, J., Sommer, J. H., Henry, E. R., & Eaton, W. A. (1983) *Proc. Natl. Acad. Sci. U.S.A. 80*, 2235.
Hofrichter, J., Henry, E. R., Sommer, J. H., Ikeda-Saito, M., Yonetani, T., & Eaton, W. A. (1985) *Biochemistry 24*, 2667−2679.
Huang, Y., & Ackers, G. K. (1995) *Biochemistry 34*, 6316−6327.
Huang, Y., & Ackers, G. K. (1996) *Biochemistry 35*, 704−718.
Huang, S., Peterson, E. S., Ho, C., & Friedman, J. M. (1997) *Biochemistry 36*, 6197−6206.
Ishimori, K., Imai, K., Miyazaki, G., Kitagawa, T., Wada, Y., Morimoto, H., & Morishima, I. (1992) *Biochemistry 31*, 3256−3264.
Jayaraman, V., & Spiro, T. G. (1996) *Biospectroscopy 2*, 311−316.
Jayaraman, V., Rodgers, K. R., Mukerji, I., & Spiro, T. G. (1995) *Science 269*, 1843−1848.
Kavanaugh, J. S., Weydert, J. A., Rogers, P. H., & Arnone, A. (1998) *Biochemistry 37*, 4358−4373.
Kiger, L., Klinger, A. L., Kwiatkowski, L. D., DeYoung, A., Doyle, M. L., Holt, J. M., Noble, R. W., & Ackers, G. K. (1998) *Biochemistry 37*, 4336−4345.
Kwiatkowski, L, D., Hui, H. L., Wierzba, A., Noble, R. W., Walder, R. Y., Peterson, E. S., Sligar, S. G., & Sanders, K. E. (1998) *Biochemistry 37*, 4325−4335.
Kitagawa, T. (1988) *Biological Application of Raman Spectroscopy* (Spiro, T. G., Ed.) Vol. III, pp 97−131, Wiley & Sons, New York.
Matsukawa, S., Mawatari, K., Yoneyama, Y., & Kitagawa, T. (1985) *J. Am. Chem. Soc. 107*, 1108−1113.
Mukerji, I., & Spiro, T. (1994) *Biochemistry 33*, 13132−13139.
Murray, L. P., Hofrichter, J., Henry, E. R., & Eaton, W. A. (1988a) *Biophys. Chem. 29*, 63−76.
Murray, L. P., Hofrichter, J., Henry, E. R., Ikeda-Saito, M., Kitagashi, K., Yonetani, T., & Eaton, W. A. (1988b) *Proc. Natl. Acad. Sci. U.S.A. 85*, 2151−2155.
Nagai, K., & Kitagawa, T. (1980) *Proc. Natl. Acad. Sci. U.S.A. 77*, 2033−2037.
Nagai, M., Kaminaka, S., Ohba, Y., Nagai, Y., Mizutani, Y., & Kitagawa, T. (1995) *J. Biol. Chem. 270*, 1636−1642.
Ondrias, M. R., Rousseau, D. L., Kitagawa, T., Ikeda-Saito, M., Inubushi, T., & Yonetani T. (1982) *J. Biol. Chem. 257*, 8766−8770.
Owen, M. C., Ockelford, P. A., & Wells, R. M. G. (1993) *Hemoglobin 17*, 513−521.
Perutz, M. F. (1989) *Q. Rev. Biophys. 22*, 139−236.
Perutz, M. F., Fermi, G., Luisi, B., Shaanan, B., & Liddington., R. C. (1987) *Acc. Chem. Res. 20*, 309−321.
Petrich, J. W., Poyart, C., & Martin, J. L. (1988) *Biochemistry 27*, 4049−4060.
Rousseau, D. L., & Friedman, J. M. (1988) *Biological Application of Raman Spectroscopy* (Spiro, T. G., Ed.) Vol. III, pp 133−215, Wiley & Sons, New York.
Scott, T. W., & Friedman, J. M. (1984) *J. Am. Chem. Soc. 106*, 5677−5687.
Scott, T. W., Friedman, J. M., Ikeda-Saito, M., & Yonetani, T. (1983) *FEBS Lett. 158*, 69−72.
Shaanan, B. (1983) *J. Mol. Biol. 171*, 31−59.
Sharma, V. J., Newton, G. L., Ranney, H. M., Ahmed, F., Harris, J. W., & Danish, E. H. (1980) *J. Mol. Biol. 144*, 267−280.
Stavrov, S. S. (1993) *Biophys. J. 65*, 1943−1950.
Vallone, B., Bellelli, A., Miele, A., Brunori, M., & Fermi, G. (1996) *J. Biol. Chem. 271*, 12472- 12480.
Yamaoka, K. (1971) *Blood 38*, 730−738.

BI9708693